Cell

PH Domain-Only Protein PHLDA3 Is a p53-Regulated Repressor of Akt

Tatsuya Kawase,[1,8,9,11] Rieko Ohki,[1,9,11,*] Tatsuhiro Shibata,[2,3] Shuichi Tsutsumi,[7] Naoko Kamimura,[7] Johji Inazawa,[6] Tsutomu Ohta,[4] Hitoshi Ichikawa,[5] Hiroyuki Aburatani,[7] Fumio Tashiro,[8] and Yoichi Taya[1,9,10]
[1]Radiobiology Division
[2]Cancer Genomics Project
[3]Pathology Division
[4]Center for Medical Genomics
[5]Cancer Transcriptome Project
National Cancer Center Research Institute, Tsukiji 5-1-1, Chuo-ku, Tokyo 104-0045, Japan
[6]Department of Molecular Cytogenetics, Medical Research Institute, Tokyo Medical and Dental University, 1-5-45 Yushima, Bunkyo-ku, Tokyo 113-8510, Japan
[7]Genome Science Division, Research Center for Advanced Science and Technology, University of Tokyo, 4-6-1 Komaba, Meguro-ku, Tokyo 153-8904, Japan
[8]Department of Biological Science and Technology, Faculty of Industrial Science and Technology, Tokyo University of Science, Yamazaki 2641, Noda-shi, Chiba 270-8510, Japan
[9]SORST/JST, Kawaguchi Center Building, 4-1-8 Honcho, Kawaguchi-shi, Saitama 332-0012, Japan
[10]Cancer Research Center of Excellence, Center for Life Sciences, #02-07, 28 Medical Drive, National University of Singapore, Singapore 117456
[11]These authors contributed equally to the work
*Correspondence: rohki@ncc.go.jp
DOI 10.1016/j.cell.2008.12.002

SUMMARY

p53 and Akt are critical players regulating tumorigenesis with opposite effects: whereas p53 transactivates target genes to exert its function as a tumor suppressor, Akt phosphorylates its substrates and transduces downstream survival signals. In addition, p53 and Akt negatively regulate each other to balance survival and death signals within a cell. We now identify *PHLDA3* as a p53 target gene that encodes a PH domain-only protein. We find that PHLDA3 competes with the PH domain of Akt for binding of membrane lipids, thereby inhibiting Akt translocation to the cellular membrane and activation. Ablation of endogenous PHLDA3 results in enhanced Akt activity and decrease of p53-dependent apoptosis. We also demonstrate the suppression of anchorage-independent cell growth by PHLDA3. Loss of the *PHLDA3* genomic locus was frequently observed in primary lung cancers, suggesting a role of PHLDA3 in tumor suppression. Our results reveal a new mode of coordination between the p53 and Akt pathways.

INTRODUCTION

Proper regulation of cell death, survival, and proliferation is fundamental to ensuring homeostasis of a multicellular organism. Complex signal transduction pathways controlled by oncoproteins and tumor suppressor proteins enable an elaborate balance of growth-promoting and growth-suppressing signals within a cell. One example of such a pathway is mutual regulatory crosstalk between tumor suppressor protein p53 and oncoprotein Akt, two key molecules regulating the life and death of a cell (Cully et al., 2006; Oren, 2003; Vousden and Prives, 2005).

The Akt signaling pathway plays a central role in cell survival and proliferation. Several components of this pathway are dysregulated in a wide spectrum of human cancers (i.e., Akt, PI3K, and PTEN), establishing its importance in oncogenesis (Luo et al., 2003). Mitogenic signals by receptor tyrosine kinases are first transmitted to phosphatidylinositol 3-kinase (PI3K), leading to production of a second messenger, phosphatidylinositol (3,4,5)-trisphosphate (PIP_3). PIP_3 generation on the inner side of the plasma membrane leads to translocation and activation of Akt. Akt activation is regulated by a dual mechanism that requires both translocation to the plasma membrane and phosphorylation at Thr308 and Ser473. Akt is recruited to the plasma membrane through direct interaction with its pleckstrin homology (PH) domain, functioning as lipid-binding modules. Downstream of Akt, Akt substrates contribute to the effects of Akt in cell survival and proliferation (Manning and Cantley, 2007).

In contrast, p53 plays a major role in the induction of growth arrest and cell death (Harris and Levine, 2005; Liu and Chen, 2006; Oda et al., 2000; Ohki et al., 2000). As the inactivation of p53 abrogates p53-mediated growth constraints, loss of functional p53 is a prerequisite for oncogenesis and is the most common anomaly in human cancers (Vogelstein et al., 2000; Vousden and Prives, 2005). Various stress signals stabilize and activate p53, which exerts its tumor-suppressive function mainly

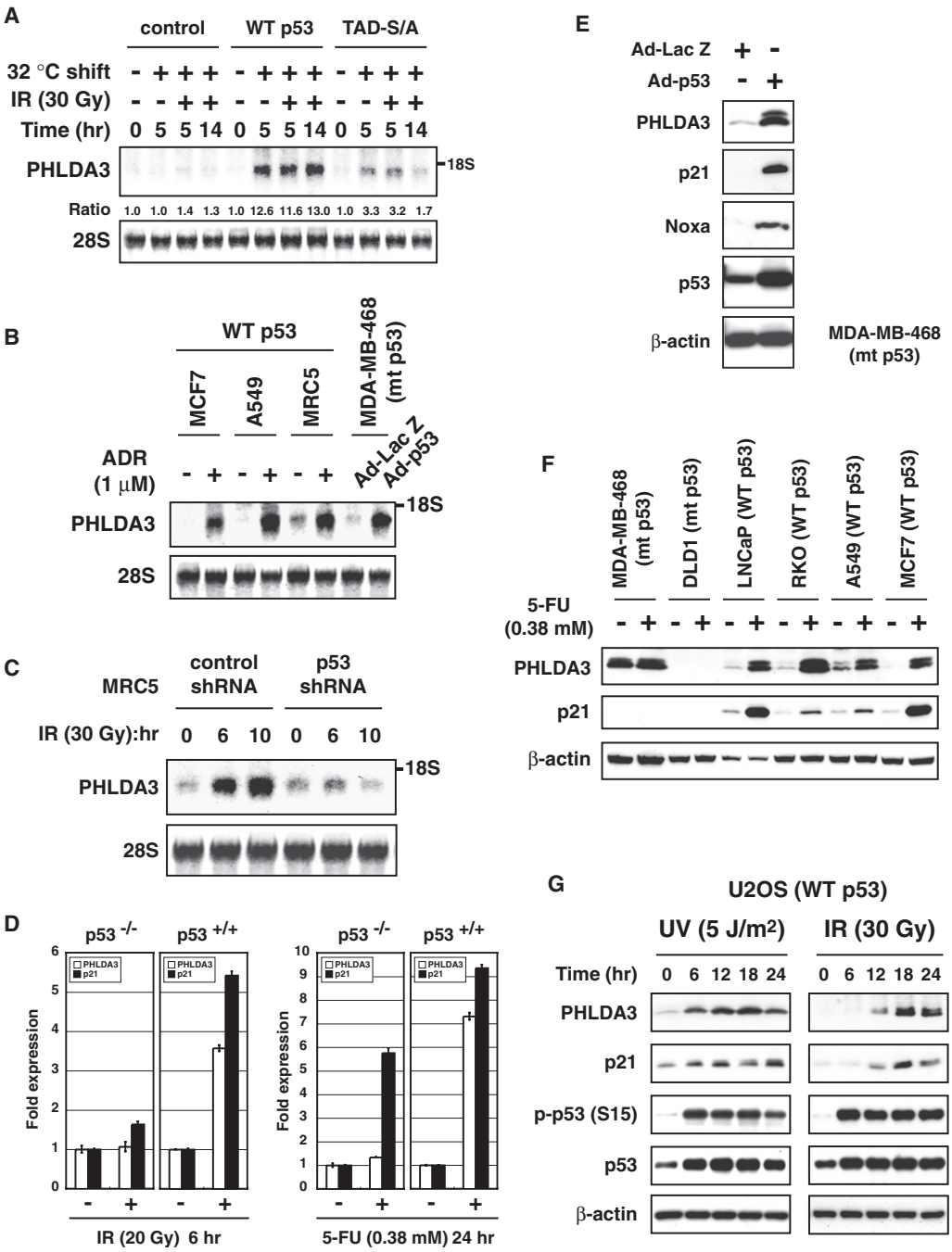

Figure 1. PHLDA3 Is Induced by p53

(A–C) PHLDA3 expression was analyzed by northern blotting. Methylene blue staining of 28S ribosomal RNA was also shown to confirm equal loading of RNA in each lane.

(A) Temperature-sensitive (ts) WT p53- or ts-TAD-S/A-expressing Saos2 cell lines were tested for PHLDA3 induction ability upon temperature shift to the permissive temperature with or without γ-ray irradiation. Cells were subjected to γ-ray irradiation 2 hr after temperature shift to 32°C. Cells were collected 5 or 14 hr post-temperature shift. Raw northern blotting data are shown in the top panel, and the relative signal intensities for PHLDA3 expression (normalized by 28S intensities) were quantified by NIH Image J software and are shown below the panel.

(B) MCF7, A549, and MRC5 cells were treated with adriamycin for 18 hr. MM468 cells were transduced with control LacZ-expressing (Ad-LacZ) or p53-expressing adenovirus (Ad-p53) at multiplicity of infection (moi) 15 and harvested 18 hr post-infection.

(C) MRC5 cells transduced with control lentivirus or lentivirus expressing p53 shRNA were subjected to γ-ray irradiation.

(D) HCT116 $p53^{+/+}$ and HCT116 $p53^{-/-}$ cells were subjected to γ-ray irradiation or 5-FU. Cells were harvested at the indicated times following treatment. RNA was purified from each sample and analyzed by quantitative real-time PCR. The mRNA levels of PHLDA3 and p21 were standardized by mRNA levels of GAPDH. All samples were run in triplicate, and data are represented as the mean fold expression ± standard deviation (SD).

as a transcriptional activator. Many p53 target genes have been identified that regulate various processes involved in the prevention of tumorigenesis, such as the induction of cell-cycle arrest, cell death, DNA repair, and senescence. It has been postulated that target genes are selectively activated to implement different p53-mediated responses, depending on the stress signal that activates p53. Posttranslational modification of p53 is the candidate mechanism that makes p53 respond to different stress signals, and phosphorylation of p53 is a major posttranslational modification of p53 (Bode and Dong, 2004). Moreover, recent studies have shown the importance of p53 phosphorylation in the induction of several p53 target genes.

Akt-p53 mutual regulation involves Akt substrates and p53 target genes; for example, one target gene of p53, *PTEN*, negatively regulates Akt (Mayo and Donner, 2002). *PTEN* encodes a phosphatase that dephosphorylates lipid PIP_3, which is essential for Akt activation. On the other hand, p53 is also negatively regulated by Akt. Akt phosphorylates Mdm2, a negative regulator of p53 that targets p53 for degradation, and Mdm2 phosphorylation leads to accelerated degradation of p53. Moreover, the *mdm2* gene is transcriptionally regulated by p53, forming a p53-Mdm2 autoregulatory feedback loop (Brooks and Gu, 2006). Thus, Akt and p53 negatively regulate each other by a complex protein network to ensure coordinated growth control within a cell.

As is evident from the findings of PTEN and Mdm2, identification of p53 target genes led to the discovery of tumor-associated genes. *PTEN* is a tumor suppressor gene mutated in breast cancers and gliomas, while *mdm2* is an oncogene frequently amplified in tumors without p53 mutations (Mayo and Donner, 2002). In order to identify genes participating in the regulation of tumorigenesis, and to dissect the functional relevance of p53 phosphorylation in target gene induction, we performed exhaustive analysis to identify p53 target genes that are induced in a manner dependent on p53 phosphorylation status (Ohki et al., 2007; Kawase et al., 2008). We found that approximately 80% of genes depended on p53 phosphorylation, showing its importance in transcriptional activity of p53. Adding to the list of previously identified genes, we report here a p53 target gene, *PHLDA3*, that encodes a PH domain-only protein that suppresses Akt activity by directly interfering with Akt binding to membrane lipids. PHLDA3 also inhibits anchorage-independent growth and is a candidate tumor suppressor of lung endocrine tumors.

RESULTS

PHLDA3 Is a Direct Target Gene of p53

Previously, we identified by microarray expression analysis genes induced by wild-type (WT) p53 and TAD-S/A, a phosphorylation-defective p53 mutant carrying point mutations at all Ser residues within the transactivation domain (TAD) (Ohki et al., 2007). As shown in Figures 1A and S1A (available online), *PHLDA3* was one of the identified genes induced by WT p53 but not by TAD-S/A. PHLDA3 transcript was also induced by exogenous expression of p53, adriamycin treatment in cells carrying WT p53, γ-ray irradiation, and 5-fluorouracil (5-FU) in a p53-dependent manner (Figures S1B, S1C, and 1B–1D). We also showed that the induction kinetics of PHLDA3 mRNA was similar to that of representative target genes of p53 (Figure S1D). In addition, PHLDA3 protein expression was induced by exogenous expression of p53 and various DNA-damaging agents, including 5-FU, ultraviolet (UV), and γ-ray irradiation, in cell lines carrying WT p53 (Figures 1E–1G and S2A–S2E). Furthermore, PHLDA3 and p21 proteins were induced with similar kinetics by UV and γ-ray irradiation (Figures 1G and S2E).

It has been reported previously that the *PHLDA3* (also named *Tih1*) gene has sequence similarity to an imprinted gene, *Ipl* (Frank et al., 1999). As shown in Figure S3, Ipl transcript was not induced with a dependence on p53, and although *PHLDA3* and *Ipl* genes share sequence homology, they are regulated in different ways.

As it had been demonstrated that *PHLDA3* is a p53-responsive gene, we then explored whether *PHLDA3* is also a direct target gene of p53. The consensus binding motif of p53 is composed of two copies of 5′-RRRCWWGYYY-3′ (R: purine, Y: pyrimidine, W: A or T) (Harris and Levine, 2005). As shown in Figure 2A, we found a putative p53-responsive element (p53RE) upstream of the *PHLDA3* gene, overlapping the transcription initiation site. Interestingly, this putative p53RE was highly conserved among the species. In order to clarify if this putative p53RE is activated by p53, the upstream region of the *PHLDA3* gene was cloned and assayed for p53 responsiveness. We first analyzed whether promoters with or without p53RE showed p53 responsiveness by luciferase reporter promoter assay. As shown in Figure 2B, p53 responsiveness strictly depended on intact p53RE. Furthermore, double-stranded synthetic oligonucleotide containing p53RE inserted upstream of the luciferase gene conferred strong p53 response on the promoter, which was abolished when p53RE was mutated (Figure 2C). On the other hand, the p53 mutant, V143A, which has no transactivation ability, did not activate the promoters, confirming that *PHLDA3* promoter activation depends on p53 transcriptional activity (Figures 2B and 2C).

We next analyzed whether p53 protein binds to the *PHLDA3* promoter in vivo. As shown in Figure 2D, binding of WT p53 and TAD-S/A to the *PHLDA3* promoter was analyzed by chromatin immunoprecipitation (ChIP) assay, and it was strengthened when both p53s were active. Furthermore, we comprehensively analyzed p53 binding near the *PHLDA3* gene, utilizing ChIP-chip and ChIP sequence technology. As shown in Figures 2E and S4A, strong and specific binding of endogenous p53 at p53RE was detected upon DNA damage. The signal obtained by ChIP-chip analysis was proportional to the strength of p53 binding, and the signal obtained for the *PHLDA3* gene was as

(E–G) Western blotting was performed to detect PHLDA3 protein expression. In all cases, PHLDA3 protein migrated as a doublet (see also Figure S2A). Expression and activation (Ser15 phosphorylation) of p53 and expressions of representative p53 target genes (p21 and Noxa) were also analyzed.
(E) MM468 cells were transduced with Ad-LacZ or Ad-p53 at moi 15 and harvested 18 hr post-infection.
(F) Indicated cells were treated with 5-FU for 20 hr. Note that neither PHLDA3 nor p21 protein is induced in cell lines carrying mutant p53.
(G) U2OS cells were treated with UV or γ-ray irradiation.

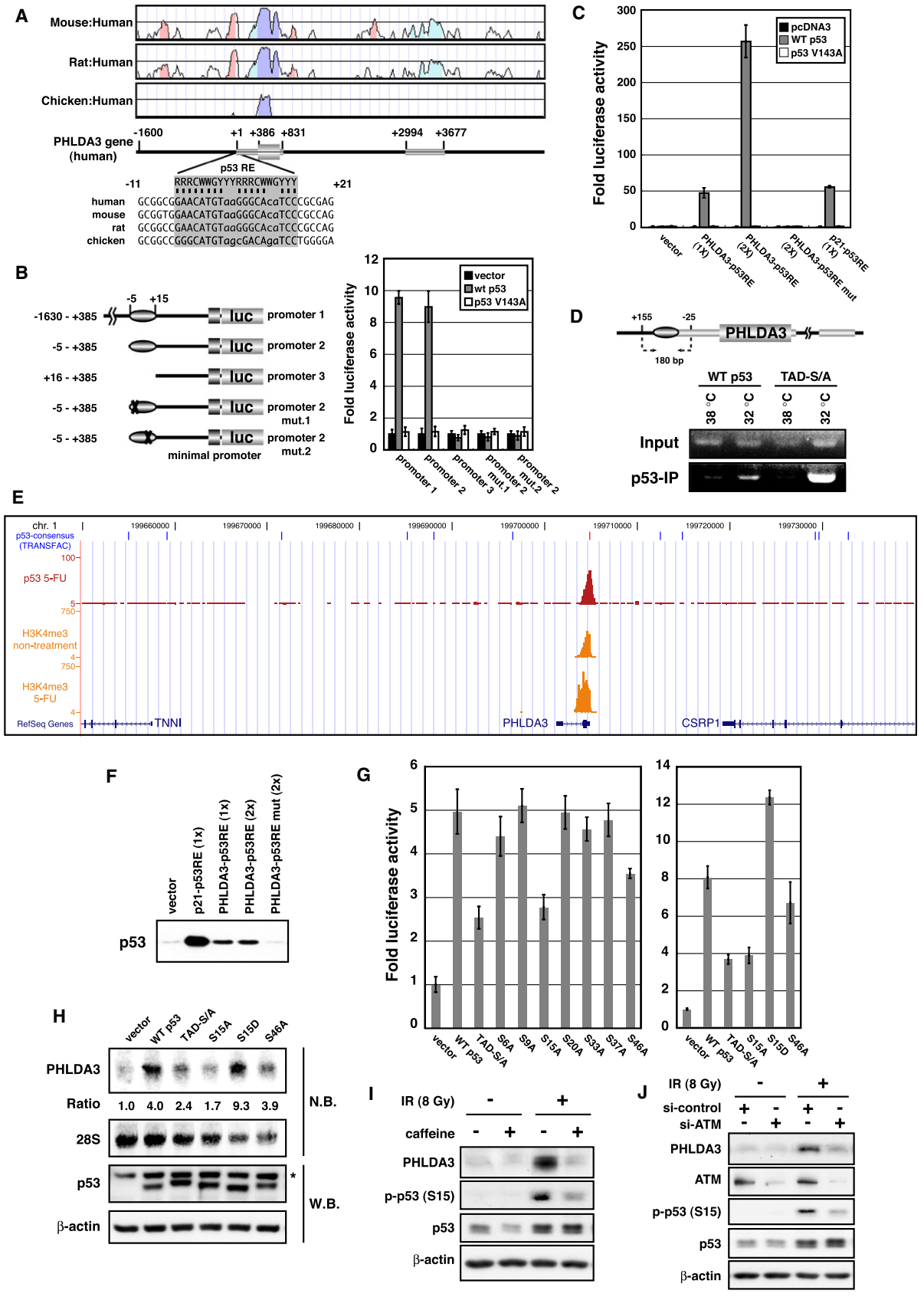
A
Mouse:Human
Rat:Human
Chicken:Human
PHLDA3 gene (human)
-1600
+1 +386 +831
+2994 +3677
p53 RE
-11
RRRCWWGYYYRRRCWWGYYY
+21
human GCGGCGGAACATGTaaGGGCAcaTCCCGCGAG
mouse GCGGTGGAACATGTaaGGGCAcaTCCCGCCAG
rat GCGGCCGAACATGTaaGGGCAcaTCCCGCCAG
chicken GCGGCCGGGCATGTagcGACAgaTCCTGGGGA
B
-5 +15
-1630 - +385 luc promoter 1
-5 - +385 luc promoter 2
+16 - +385 luc promoter 3
-5 - +385 luc promoter 2 mut.1
-5 - +385 luc promoter 2 mut.2
minimal promoter
Fold luciferase activity
vector
wt p53
p53 V143A
promoter 1
promoter 2
promoter 3
promoter 2 mut.1
promoter 2 mut.2
C
Fold luciferase activity
pcDNA3
WT p53
p53 V143A
vector
PHLDA3-p53RE (1X)
PHLDA3-p53RE (2X)
PHLDA3-p53RE (2X)
PHLDA3-p53RE mut (1X)
p21-p53RE (1X)
D
+155
-25
PHLDA3
180 bp
WT p53
TAD-S/A
38 °C
32 °C
38 °C
32 °C
Input
p53-IP
E
chr. 1
199660000
199670000
199680000
199690000
199700000
199710000
199720000
199730000
p53-consensus (TRANSFAC)
p53 5-FU
H3K4me3 non-treatment
H3K4me3 5-FU
RefSeq Genes
TNNI
PHLDA3
CSRP1
F
vector
p21-p53RE (1x)
PHLDA3-p53RE (1x)
PHLDA3-p53RE (2x)
PHLDA3-p53RE mut (2x)
p53
G
Fold luciferase activity
vector
WT p53
TAD-S/A
S6A
S9A
S15A
S20A
S33A
S37A
S46A
vector
WT p53
TAD-S/A
S15A
S15D
S46A
H
vector
WT p53
TAD-S/A
S15A
S15D
S46A
PHLDA3
Ratio 1.0 4.0 2.4 1.7 9.3 3.9
N.B.
28S
p53
*
W.B.
β-actin
I
IR (8 Gy) - +
caffeine - + - +
PHLDA3
p-p53 (S15)
p53
β-actin
J
IR (8 Gy) - +
si-control + - + -
si-ATM - + - +
PHLDA3
ATM
p-p53 (S15)
p53
β-actin

strong as other representative p53 target genes (Figure S4B). In addition, quantitative PCR was performed to analyze p53RE enrichment by ChIP. The relative enrichment of *PHLDA3* p53RE after ChIP was compared to a locus with no p53 binding and was concentrated more than 50-fold (Figure S4C). Moreover, ChIP sequence assay was performed for histone H3 trimethylated at Lys 4 (trimethyl K4/H3). It has been reported that trimethyl K4/H3 peaks in the 5′ transcribed region and active genes can be discriminated from inactive genes by high levels of trimethyl K4/H3 (Schneider et al., 2004). Upon DNA damage, the *PHLDA3* gene was actively transcribed and increased trimethyl K4/H3 was detected in the 5′ transcribed region simultaneously (Figures S1D and 2E). We finally analyzed, by p53 pull-down assay using biotinylated DNA probes containing one or two copies of p53RE, whether p53 binds directly to p53RE. As shown in Figure 2F, p53 was pulled down by WT but not by mutant p53RE. Collectively, these results identify *PHLDA3* as a bona fide target gene of p53 and p53RE as the p53-responsive element of the *PHLDA3* gene.

PHLDA3 Expression Is Regulated by p53 Phosphorylation Status

Multiple phosphorylation occurs within the TAD of p53 and regulates p53 transcriptional activity (Bode and Dong, 2004). As shown in Figures 1A and 2G, we found that PHLDA3 expression and promoter activation was severely diminished in cells expressing TAD-S/A. We therefore analyzed which Ser residue within the TAD contributes to PHLDA3 expression. We constructed p53 phosphorylation-deficient mutants carrying single amino acid conversions from Ser to Ala on all Ser residues within the TAD. As shown in Figure 2G, while p53 Ala mutants at Ser6, 9, 20, 33, and 37 showed activity similar to WT p53, the mutant at Ser15 showed decreased activity, similar to TAD-S/A. In addition, phosphorylation-mimic mutant S15D showed enhanced promoter response (Figure 2G, right panel). The requirements for Ser15 phosphorylation were also confirmed by analyzing endogenous PHLDA3 transcriptional activation by WT p53, TAD-S/A, S15A, S15D, or S46A (Figure 2H) and by mutants carrying combined (S15, 20A and S6, 33, 46A) amino acid conversions (Figure S5A). On the other hand, although weak impairment of *PHLDA3* promoter activation was observed for S46A (Figure 2G left panel), it was not observed for endogenous PHLDA3 induction (Figures 2H and S5A).

Phosphorylation of Ser15 upon genotoxic stress is dependent on ATM (Bode and Dong, 2004). Upon γ-ray irradiation, efficient Ser15 phosphorylation and PHLDA3 expression were detected, whereas both were diminished in the same cells treated with caffeine, an ATM inhibitor (Figure 2I). Furthermore, when cells were treated with siRNA targeting ATM, Ser15 phosphorylation and PHLDA3 expression reduced simultaneously upon γ-ray irradiation (Figure 2J). We also analyzed PHLDA3 expression in ATM-proficient normal human fibroblast WI-38 and ATM-deficient AT2KY fibroblasts and showed that ATM is required for both Ser15 phosphorylation and PHLDA3 expression (Figures S5B and S5C). These results collectively support the idea that p53 activation upon DNA damage is regulated by Ser15 phosphorylation, and PHLDA3 expression is dependent on it. ChIP analysis results showed that TAD-S/A can bind to the *PHLDA3* promoter as efficiently as WT p53 (Figure 2D); however, TAD-S/A is unable to fully activate the *PHLDA3* promoter. The phosphorylation status of p53 may not affect p53 binding to the *PHLDA3* promoter

Figure 2. *PHLDA3* Is a Direct Target Gene of p53

(A) Genomic organization of *PHLDA3* (chr1: 198, 164, 473–198, 171, 696) is shown together with the plots of pairwise genomic alignments between human and mouse, human and rat, and human and chicken. Genomic alignment plots were constructed using VISTA (http://genome.lbl.gov/vista/index.shtml). Based on genomic alignments, nucleotide conservation was calculated with a 100 bp window, and conservation percentage is shown as a plot. The position and nucleotide sequence of p53-responsive element are shown at the bottom.

(B) *PHLDA3* promoter region with or without p53RE (shown as an oval) was cloned upstream of firefly luciferase reporter gene with a minimal promoter, and luciferase reporter assay was performed. Constructs contain indicated positions relative to the transcription initiation site. Nucleotides that matched p53 consensus binding sites, 4th and 7th nucleotides for promoter 2 mut.1 and 14th nucleotide for promoter 2 mut.2, were mutated. Constructs were tested for transactivation by WT p53 and p53-V143A. The assay was performed 24 hr post-transfection. The experiment was run in triplicate, and data are represented as the mean fold activation ± SD.

(C) One or two copies of double-stranded synthetic oligonucleotide containing p53RE were inserted into the luciferase repoter plasmid containing a minimal promoter. The assay was performed as in (B).

(D) ChIP assay was performed for the *PHLDA3* promoter. The ts WT p53- and TAD-S/A-expressing Saos2 cell lines were used to analyze p53 binding to the *PHLDA3* promoter upon temperature shift to the permissive temperature. The positions of PCR primers within the *PHLDA3* promoter region are shown at the top.

(E) HCT116 $p53^{+/+}$ cells were treated with 5-FU, and p53 ChIP-chip or trimethyl K4/H3 ChIP sequence analysis was performed. Genomic locus of *PHLDA3* is shown together with the results obtained. Vertical axis shows the probability value (-log P), which reflects the fold enrichment of ChIP-chip or ChIP sequence samples. Blue and red lines at the top indicate the p53-consensus region computed from TRANSFAC analysis. One p53-consensus region matched completely with p53RE obtained from our analysis (shown by a red line).

(F) p53 pull-down using biotinylated DNA probes was performed. Two additional DNA probes served as controls: one containing the *p21*-derived sequence (p21-p53RE) as a positive control and another containing a nonrelevant sequence derived from a plasmid as a negative control. Bound p53 was analyzed by western blotting.

(G–J) Full activation of the *PHLDA3* promoter requires p53 phosphorylation, especially at Ser15.

(G) Luciferase assay was performed as in (B) using promoter 2. Saos2 cells were transfected with the indicated constructs and promoter 2 and analyzed 48 hr post-transfection.

(H) Endogenous PHLDA3 expression was analyzed by northern blotting. Saos2 cells were transfected with the indicated p53s and harvested 24 hr post-transfection. Relative signal intensities for PHLDA3 expression were quantified as in Figure 1A and are shown below the panel. p53 protein levels were analyzed and are shown in the bottom panel. Asterisk denotes a nonspecific band detected by anti-p53 polyclonal antibody.

(I) MCF7 cells were subjected to γ-ray irradiation with or without caffeine. Caffeine was added to the medium 1 hr prior to γ-ray irradiation. Cells were harvested 4 hr post-irradiation. Western blotting was performed to detect p53 expression and activation (Ser15 phosphorylation of p53).

(J) MCF7 cells were transfected with siRNA targeting ATM and analyzed as in (I).

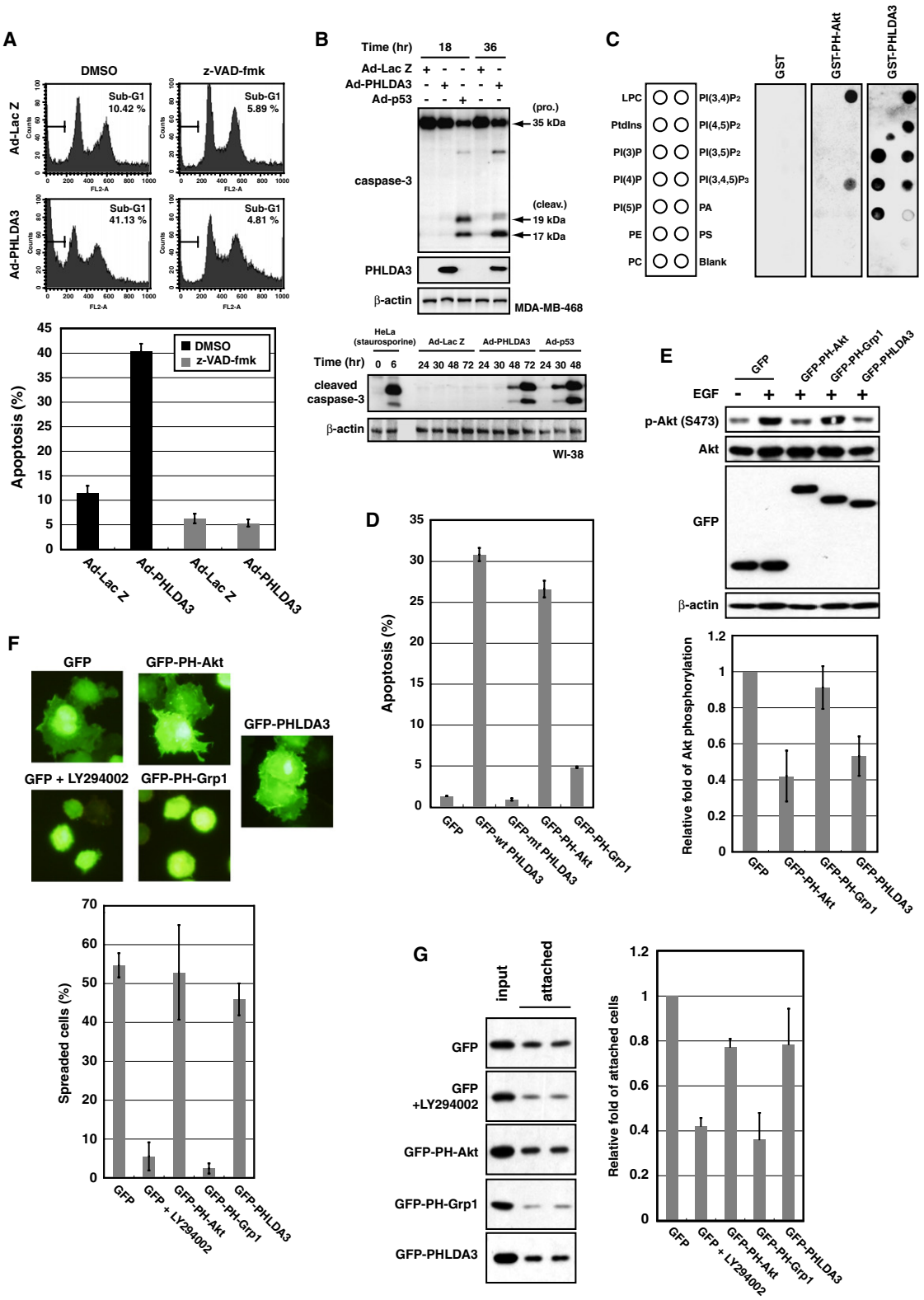

Figure 3. PHLDA3 Induces Apoptosis and Represses Akt

(A) PHLDA3 induces caspase-dependent cell death. MM468 cells were transduced with Ad-LacZ or N-terminally HA-tagged PHLDA3-expressing adenovirus (Ad-PHLDA3) at moi 15. Cells were cultured with or without caspase-specific peptide inhibitor z-VAD-fmk. Cells were harvested 48 hr post-infection and analyzed by FACS. Percentages of cells with sub-G1 DNA content are shown (bottom panel).

but may affect other aspects of *PHLDA3* promoter activation, such as cofactor recruitment to the promoters, leading to its efficient activation.

PHLDA3 Is an Apoptosis Inducer

To explore the physiological functions of PHLDA3, we first transduced PHLDA3 by adenovirus-mediated gene transfer and analyzed the effect of ectopic PHLDA3 expression. As shown in Figures S6A and S9B, PHLDA3 induced cell death in several cell lines irrespective of the p53 status, consistent with PHLDA3 as a downstream mediator of p53. We found that cells with sub-G1 DNA content were increased by PHLDA3 expression (Figure S6A), and this increase was inhibited by z-VAD-fmk addition, a specific caspase inhibitor, showing that PHLDA3-induced cell death is caspase dependent (Figure 3A). In addition, caspase 3 activation and increased annexin V-positive/PI-negative cells were observed upon PHLDA3 expression (Figures 3B and S6B). We also compared the cell death-inducing ability of PHLDA3 with that of p53 and Noxa, a representative p53 target gene that induces apoptosis (Figure S6C). Although cell-death induction was weaker than that with p53, PHLDA3 induced cell death similarly to Noxa. Besides, we showed that endogenous PHLDA3 is required for p53-dependent apoptosis (Figure 5, discussed in detail later). Collectively, it was shown that PHLDA3 expression leads to apoptosis induction.

PHLDA3 Induces Apoptosis through Its PH Domain

PHLDA3 protein is highly conserved in vertebrates and is a small protein of 127 aa mostly comprised of the PH domain (Figure S7). Based on the results of the in vitro phosphatidylinositol phosphate (PIP) binding assay, the PH domain of PHLDA3 is functional and binds to most PIP (Figure 3C and Saxena et al., 2002). PHLDA3 binding to PIP occurs without stimulation and therefore PHLDA3 is localized to the cellular membrane when expressed (Figure S8). Accordingly, we tested whether PHLDA3's ability to induce apoptosis is dependent on the function of its PH domain. We fused WT PHLDA3 (WT PHLDA3) and mtPHLDA3, a PHLDA3 mutant with a small deletion within the PH domain (Figure S7), with GFP or DsRed, and subcellular localization was analyzed. As shown in Figures 4C and 4D, while DsRed-WT PHLDA3 localized to the plasma membrane as expected, DsRed-mtPHLDA3 localized mainly in the cytoplasm, showing that the PH domain of mtPHLDA3 is nonfunctional (equivalent GFP fusion proteins showed the same subcellular localizations, Figure 3F and data not shown). We next expressed GFP, GFP-WT PHLDA3, and GFP-mtPHLDA3 in 293T cells and analyzed GFP-positive cells by flow cytometry. As shown in Figure 3D, compared to GFP-expressing cells, an increase of dead cells was observed in cells expressing GFP-WT PHLDA3, while no increase was observed for cells expressing GFP-mtPHLDA3. These results demonstrate that the functional PH domain is required for PHLDA3-induced apoptosis.

PHLDA3 Acts Similarly to the PH Domain of Akt

The PH domain is an approximately 100-residue protein module found in many signaling proteins and binds to PIP located on the inner plasma membrane. The PH domain mediates protein recruitment to cellular membranes, which is of paramount importance for signal transduction (Lemmon and Ferguson, 2000). Given that apoptosis induction of PHLDA3 requires its PH domain, and PHLDA3 has no distinct functional domain other than the PH domain, we speculated that the physiological role of PHLDA3 is to function as a PH domain-only protein. We hypothesized that PHLDA3 is induced by p53 under stressed conditions, functioning as a dominant-negative molecule for other PH domain-containing proteins to shut off the signal transduction pathway mediated by those proteins. In order to test our hypothesis, we tested whether PH domains derived from other PH domain-containing proteins function similarly to PHLDA3 within the cell. We selected two well-known PH domain-containing proteins with distinct functions within the cell: serine/threonine kinase Akt, the main molecule that transduces survival signaling, and Grp1, a member of the GTP-binding protein exchange factor family that regulates cell adhesion and spreading (Lemmon and Ferguson, 2000). It has been reported that both PH domains of Akt and Grp1 bind to PIP_3, and when isolated PH domains are expressed in cells, they function as dominant-negative forms of the proteins (Songyang et al., 1997; Varnai et al., 2005). The PH domain of Akt or Grp1 was fused with GFP (GFP-PH-Akt, GFP-PH-Grp1) and expressed in 293T and COS7

(B) Cleavage and activation of caspase 3 upon PHLDA3 expression. MM468 and WI-38 cells were transduced with Ad-LacZ, Ad-PHLDA3, or Ad-p53 at moi 35. Cells were harvested at the indicated times post-infection. HeLa cells treated with staurosporine for 6 hr were shown as a positive control for caspase 3 activation. PHLDA3 expression was detected with anti-HA antibody. Caspase 3 activation induced by PHLDA3 followed that by p53.

(C) Binding of GST-PHLDA3, GST-PH-Akt, or GST to immobilized PIP was assessed by protein-lipid overlay assay. Nitrocellulose membranes spotted with 100 pmol of different phospholipids were used for the assay. Bound proteins were detected with anti-GST antibody. Note that GST produced no signal under the conditions employed.

(D) 293T cells were transfected with GFP, GFP-WT PHLDA3, GFP-mtPHLDA3, GFP-PH-Akt, or GFP-PH-Grp1 and analyzed for GFP-positive cells 48 hr post-transfection. The apoptotic rate, measured by PI-positive cells (cells stained with PI without fixation), is shown. Mean apoptotic rates ± SD from three experiments are shown.

(E) PHLDA3 inhibits Akt activation. COS7 cells were transfected with the indicated fusion proteins for 24 hr and subsequently stimulated with EGF for 5 min. Induction of Akt phosphorylation was detected in control cells expressing GFP upon EGF treatment. Akt activity after EGF treatment was analyzed by western blotting, and Akt activity relative to the GFP-transfected control was calculated. The mean ± SD from three experiments is shown. GFP fusion protein levels were also analyzed by western blotting.

(F) Cell spreading is not inhibited by PHLDA3. The cell-spreading assay was performed. LY294002 was added 10 min before re-plating. More than 150 cells were counted from three fields, and the percentages of fully spread cells are shown. Note that PI3K inhibitor LY294002 inhibited cell spreading under the conditions tested. Mean percentage ± SD from three fields is shown. Representative images of cells are shown on the left.

(G) Cell attachment is only weakly inhibited by PHLDA3. Cell attachment assay was performed. Attached cells were harvested and analyzed by western blotting. The fraction of attached cells relative to input cells was calculated for each construct. LY294002 (added 10 min before plating) inhibited cell attachment under the conditions tested. Representative result is shown on the left, and the mean ± SD from four experiments is shown.

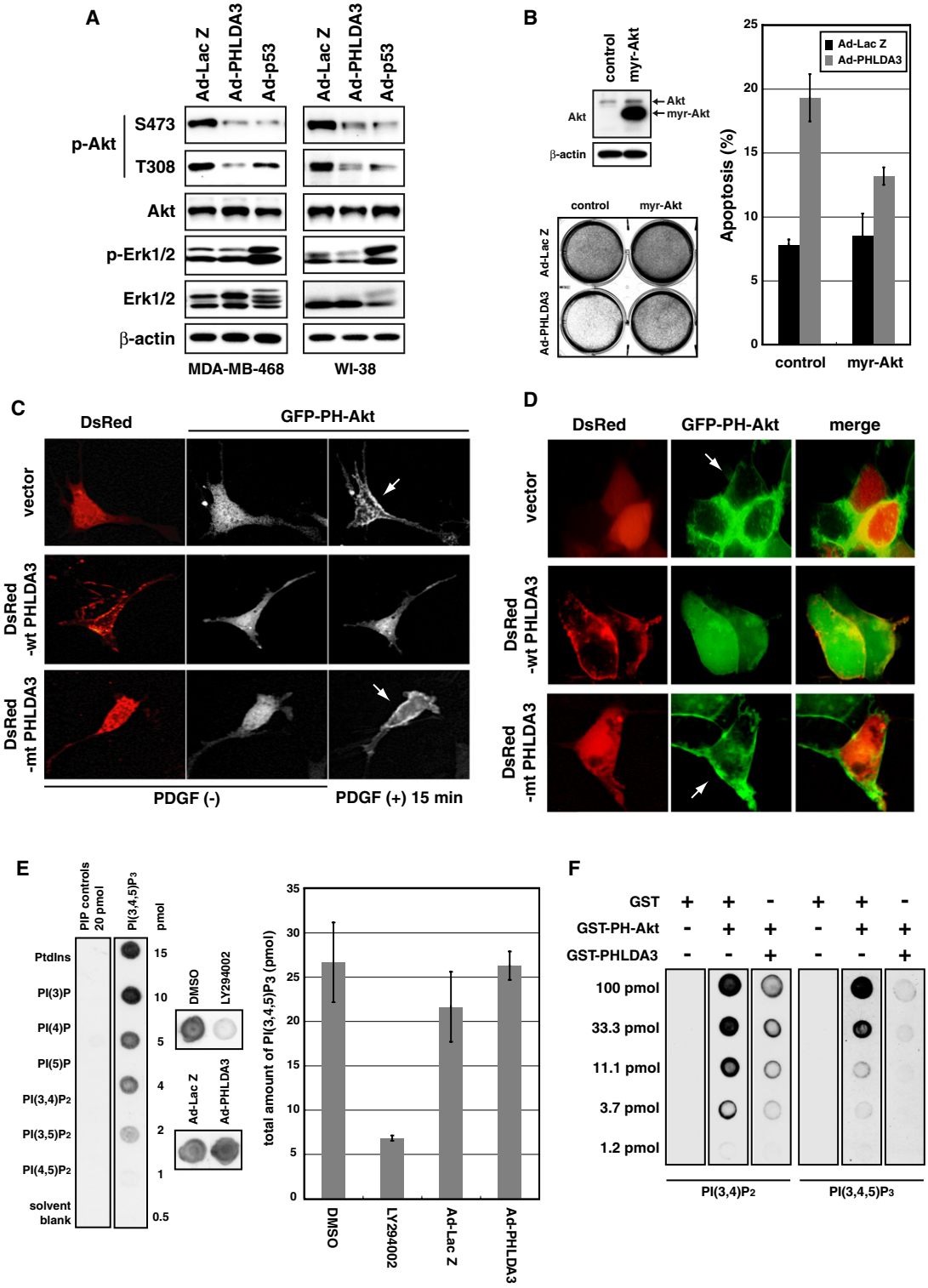

Figure 4. PHLDA3 Interferes with Akt Activation by Inhibiting Akt Binding to PI(3,4)P_2 and PI(3,4,5)P_3

(A) Indicated cells were infected with Ad-LacZ, Ad-p53, or Ad-PHLDA3 at moi 35 and analyzed 18 hr post-infection, when apoptotic cells were not yet detected. Akt and Erk activities were assessed by analyzing phosphorylated Akt and Erk1/2 by western blotting.

(B) Constitutively active Akt represses apoptosis induced by PHLDA3. MM468 cells stably expressing myr-Akt or control cells expressing only the Bsr drug resistance gene were infected with Ad-LacZ or Ad-PHLDA3 at moi 15. Myr-Akt was detected with anti-Akt antibody. Cells were fixed and stained with Giemsa 48 hr post-infection (left lower panel). Cells in sub-G1 were also analyzed by FACS (right panel). The data are represented as the mean ± SD for triplicate samples.

cells. As expected, GFP-PH-Akt repressed Akt activity and induced apoptosis by inhibition of the Akt pathway (Figures 3D and 3E), whereas GFP-PH-Grp1 inhibited cell spreading on fibronectin and cell attachment to culture dishes by inhibiting endogenous Grp1 signaling (Figures 3F and 3G). GFP-PH-Akt had no effect on cell spreading and a very weak effect on cell attachment (Figures 3F and 3G), and GFP-PH-Grp1 had a very weak effect on cell survival and no effect on Akt activity (Figures 3D and 3E), showing the selective effect of these PH domains, as reported (Varnai et al., 2005). We found that GFP-WT PHLDA3 induced apoptosis and repressed Akt activity as GFP-PH-Akt, whereas it had a very weak effect on cell spreading and attachment, showing that PHLDA3 functions similarly to the PH domain of Akt (Figures 3D–3G).

PHLDA3 Induces Apoptosis by Inhibiting Akt Activity

PHLDA3 represses Akt activity and induces apoptosis, suggesting that it functions as a PH domain-only protein to inhibit Akt; therefore, we further examined whether PHLDA3 induces apoptosis by inhibiting Akt activation. As shown in Figure 4A, PHLDA3 expression resulted in diminished Akt phosphorylation at Ser473 and Thr308, both of which are essential for Akt activity, whereas the phosphorylation status of Erk was not changed by PHLDA3 expression, showing that inhibition of Akt activity is not a result of inhibition of the global cell survival signaling pathway. We also compared sensitivity to apoptosis induction by LY294002, a specific PI3K/Akt signaling pathway inhibitor, and apoptosis by PHLDA3 expression within several cell lines (Figures S9A and S9B). Cell lines sensitive to LY294002 treatment were also sensitive to PHLDA3 expression. Furthermore, when MM468 cells were treated with LY294002, PHLDA3 expression did not enhance apoptosis, indicating that PHLDA3 expression does not increase PI3K pathway inhibition in apoptosis induction (Figure S9C). These results collectively suggest that apoptosis induction by PHLDA3 is mediated by inhibition of the PI3K/Akt pathway.

We next tested whether the expression of constitutively active forms of Akt restrains apoptosis induced by PHLDA3. We selected two constitutively active forms of Akt, neither of which require PIP_3 binding for activation: a double mutant mimicking phosphorylated Akt (T308D/S473D-Akt) and myristoylated and PH domain-deleted constitutively active Akt (myr-Akt). We first transfected 293T cells with GFP-PHLDA3 and T308D/S473D-Akt. As shown in Figure S10A, by cotransfection of T308D/S473D-Akt, PHLDA3-induced apoptosis was rescued, and this rescue was dependent on T308D/S473D-Akt dosage. When the effect of T308D/S473D-Akt on apoptosis induced by PHLDA3 and PH-Akt was compared, T308D/S473D-Akt similarly rescued both (Figure S10B). We next obtained cells stably expressing myr-Akt and analyzed apoptosis induction by ectopic PHLDA3 expression. As shown in Figure 4B, compared to control cells, apoptotic cells decreased and viable cells increased in myr-Akt-expressing cells, showing that myr-Akt efficiently repressed apoptosis induced by PHLDA3. Thus, these results reveal that PHLDA3 inhibits Akt activation, and Akt inhibition mainly contributes to apoptosis induction by PHLDA3.

PHLDA3 Interferes with Akt Translocation to the Plasma Membrane

Activation and phosphorylation of Akt require prior PIP binding at the plasma membrane (Stokoe et al., 1997). When $PI(3,4,5)P_3$ and $PI(3,4)P_2$ are generated by PI3K upon growth stimulation, Akt translocates from the cytoplasm to the plasma membrane by binding to PIP through its PH domain, which specifically binds to $PI(3,4,5)P_3$ or $PI(3,4)P_2$ (Figure 3C and Scheid and Woodgett, 2003). Since two constitutively active forms of Akt that do not require PIP binding for activation rescued PHLDA3-induced apoptosis, it was suggested that PHLDA3 inhibits Akt binding to PIP. We therefore analyzed whether PHLDA3 expression inhibits Akt translocation to the plasma membrane upon PIP_3 production. We coexpressed DsRed or DsRed-WT PHLDA3 together with GFP-PH-Akt in NIH 3T3 cells (Figures 4C and S11A). GFP-PH-Akt has been shown to mimic Akt translocation upon PI3K pathway activation (Harriague and Bismuth, 2002). As has been reported, PDGF treatment of control cells expressing DsRed resulted in GFP-PH-Akt translocation to the plasma membrane, whereas in cells expressing DsRed-WT PHLDA3, GFP-PH-Akt translocation was inhibited. Moreover, inhibition was not observed in cells expressing DsRed-mtPHLDA3, a PHLDA3 mutant with a defective PH domain, which cannot localize at the plasma membrane. To assess the effect of PHLDA3 expression on Akt localization in other cell lines, a similar experiment was performed using 293T cells with constitutively active PI3K activity. Again in 293T cells, DsRed-WT PHLDA3 interfered with GFP-PH-Akt localization to the plasma membrane, while DsRed or DsRed-mtPHLDA3 did not (Figures 4D and S11B). Taken together, the results show that PHLDA3 impedes Akt translocation to the cellular membrane and subsequent activation in a manner dependent on its PH domain function.

PHLDA3 Directly Interferes with Akt Binding to PIP_2 and PIP_3

Because PHLDA3 expression led to the inhibition of Akt translocation to the plasma membrane and subsequent phosphorylation and activation, we next analyzed the mechanism by which PHLDA3 inactivates Akt. We first tested whether PHLDA3

(C) Akt translocation to the plasma membrane upon PDGF treatment was analyzed by live-cell imaging. NIH 3T3 cells were transfected with GFP-PH-Akt together with DsRed, DsRed-WT PHLDA3, or DsRed-mtPHLDA3. GFP-PH-Akt subcellular localization was monitored before and after PDGF treatment (15 min). Note that Akt is localized at the plasma membrane in cells expressing DsRed or DsRed-mtPHLDA3 (shown by arrows).

(D) Akt subcellular localization in 293T cells with the constitutively active PI3K/Akt pathway. 293T cells were transfected with GFP-PH-Akt together with DsRed, DsRed-WT PHLDA3, or DsRed-mtPHLDA3, and GFP-PH-Akt subcellular localization was analyzed. Arrows indicate Akt localized at the plasma membrane.

(E) Quantification of PIP_3 in cells expressing PHLDA3. Amount of PIP_3 was quantified in lipids extracted from MM468 cells infected with Ad-LacZ and Ad-PHLDA3 and cells treated with LY294002. The data are represented as the mean ± SD from three experiments.

(F) PHLDA3 inhibits PH-Akt binding to PIP_2 and PIP_3. Binding of GST-PH-Akt to immobilized PIP was assessed by protein-lipid overlay assay. Nitrocellulose membranes spotted with serially diluted PIP_2 and PIP_3 were incubated with the indicated proteins. While GST did not interfere with Akt binding to PIP, PHLDA3 significantly interfered. Bound Akt was detected with anti-Akt PH domain antibody.

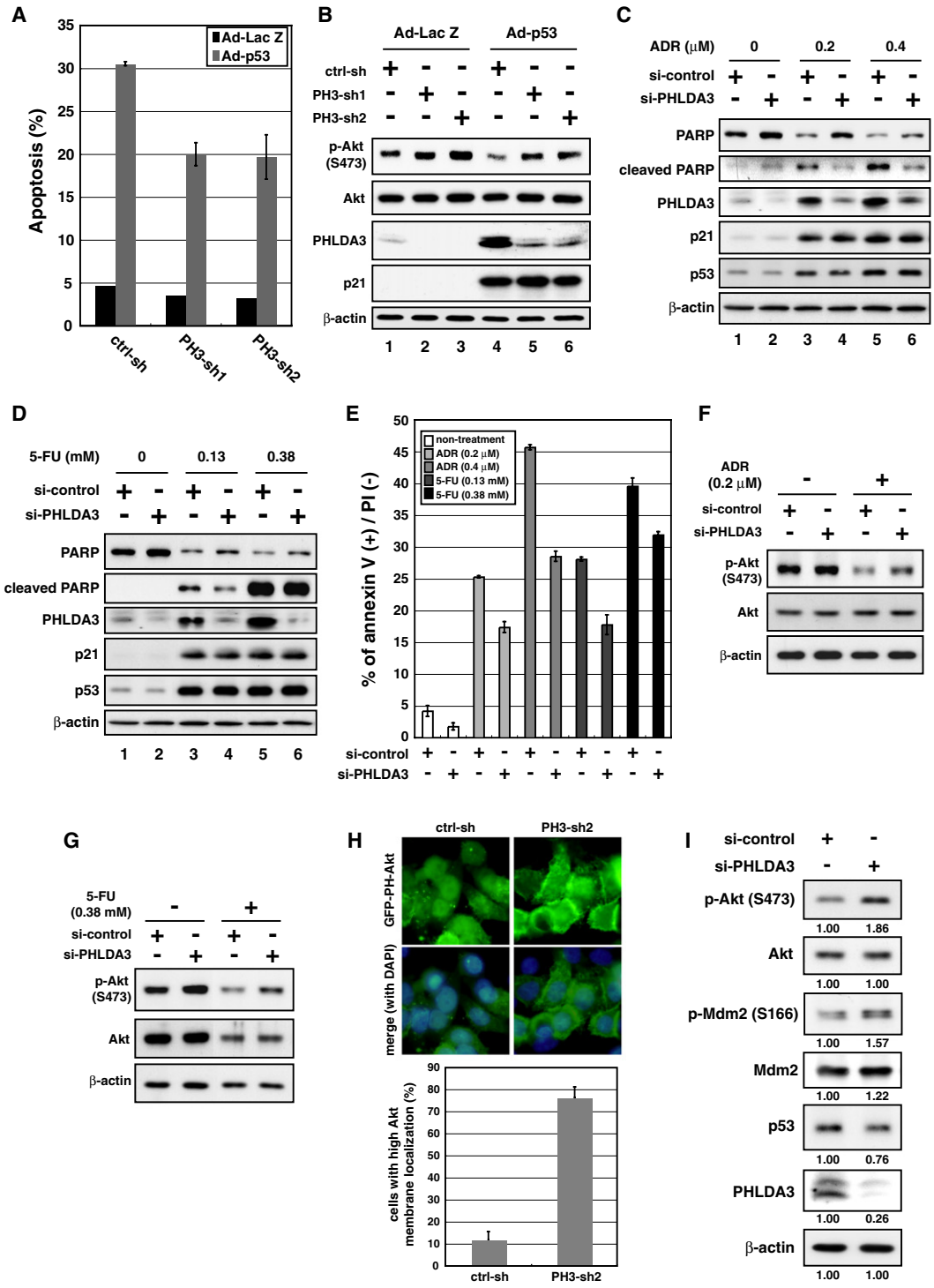

Figure 5. PHLDA3 Is Required for p53-Dependent Apoptosis

(A and B) Downregulation of PHLDA3 results in decreased p53-dependent apoptosis and elevated Akt phosphorylation. Ctrl-sh, PH3-sh1, and PH3-sh2 cells were infected with Ad-p53 at moi 3 (in A) or moi 1 (in B). Apoptotic cells as determined by cells with sub-G1 DNA content were analyzed 43 hr post-infection, and the mean ±SD for triplicate samples is shown (A). In (B), cells were treated with z-VAD-fmk to protect Akt from p53-dependent Akt degradation. Cells were harvested 50 hr post-infection and analyzed by western blotting.

(C–G) Control or PHLDA3-targeting siRNAs were introduced into LNCaP cells. Cells were treated with adriamycin or 5-FU 30 hr post-transfection. Cells were harvested 42 hr (C–E and G) or 36 hr (F) post-treatment and analyzed by western blotting (C, D, F, and G) or by FACS for annexin V-positive/PI-negative cells (E). The mean ± SD for triplicate samples is shown.

inhibits Akt activity by affecting upstream signals of Akt. Since PI3K-produced PIP_3 is essential for Akt activation, we analyzed the amount of PIP_3 in cells expressing PHLDA3 using the PIP_3 mass strip kit. Acidic lipids were extracted from MM468 cells infected with Ad-LacZ and Ad-PHLDA3 and blotted onto a PIP_3 strip. PIP_3 was quantified by detecting membrane-blotted acidic lipids with a PIP_3 detector. As shown in Figure 4E, no difference in the amount of PIP_3 was detected between control and PHLDA3-expressing cells, while significantly reduced PIP_3 was detected in MM468 cells treated with LY294002. As PHLDA3 did not affect Akt upstream signals, we next tested whether PHLDA3 physically interacts with Akt to inhibit Akt binding to PIP. HA-tagged Akt and GFP-PHLDA3 or GFP-Akt were coexpressed and immunoprecipitated with anti-HA antibody and analyzed to identify direct interaction between the proteins (Figure S12). Although Akt homodimerization was detected, as previously reported (Franke et al., 1997), no interaction between PHLDA3 and Akt was observed. We finally performed an in vitro protein-lipid overlay assay to see if PHLDA3 directly interferes with Akt binding to PIP (Figure 4F). PHLDA3 and Akt were mixed in a molar ratio of 1:1 and reacted with $PI(3,4,5)P_3$ and $PI(3,4)P_2$ to test whether PHLDA3 competitively interferes with Akt binding to PIP. As shown in Figure 4F, Akt binding to PIP was significantly inhibited by PHLDA3 but not when Akt was mixed with control GST. Collectively, these results demonstrate that PHLDA3 does not change the amount of PIP_3 within the cell or interact physically with Akt but does repress Akt activity by competitively binding to PIP.

PHLDA3 Contributes to p53-Dependent Apoptosis and Repression of Akt

We next examined whether PHLDA3 contributes to p53-depedent apoptosis. We stably knocked down PHLDA3 in MM468 cells by introducing two different shRNAs (PH3-sh1 and PH3-sh2) that efficiently knocked down PHLDA3 expression (Figures S1C, S2B, and S14B). As shown in Figure S2B, induction of p21 or Noxa by p53-expressing adenovirus (Ad-p53) did not differ among ctrl-sh, PH3-sh1, and PH3-sh2 cells, showing that the p53 pathway is normal except for PHLDA3 induction in PH3-sh1 and PH3-sh2 cells. Using these cell lines, the efficacy of p53-dependent apoptosis induced by Ad-p53 infection was analyzed. Apoptosis was not observed in cells infected with control LacZ-expressing adenovirus (Ad-LacZ), whereas Ad-p53 induced apoptosis in ctrl-sh cells; however, apoptosis by Ad-p53 was significantly diminished in PH3-sh1 and 2 cells (Figure 5A).

Inhibition of the survival signaling pathway by Akt is important for p53-dependent apoptosis (Stambolic et al., 1999), and repression of Akt activity was observed upon p53 expression in MM468 cells (Figures 4A and 5B, lane 4). It has been proposed that p53-dependent inhibition of the Akt pathway is mediated by PTEN or caspase (Oren, 2003); however, as MM468 cells do not have functional PTEN and no degradation of Akt is detected, Akt repression by p53 detected here is independent of caspase and PTEN. These results suggest a novel Akt-repressing pathway downstream of p53. We therefore analyzed whether PHLDA3 acts downstream of p53 to repress Akt. As shown in Figure 5B, in Ad-p53 infected cells, PH3-sh cells showed elevated Akt phosphorylation compared to ctrl-sh cells, demonstrating the involvement of PHLDA3 in p53-dependent repression of Akt (lanes 4–6). All cells infected with Ad-p53 showed lower Akt phosphorylation levels than equivalent cells infected with Ad-LacZ, at least partially because of residual PHLDA3 induction by p53 in PH3-sh cells. Notably, PHLDA3 expression levels had a reverse correlation with Akt phosphorylation levels. Cells with high PHLDA3 expression had very low levels of activated Akt (lane 4), cells with moderate PHLDA3 expression had medium levels (lanes 1, 5, and 6), and cells with very low PHLDA3 expression had high levels (lanes 2 and 3).

We further analyzed involvement of PHLDA3 in p53-dependent apoptosis and Akt repression induced by DNA damage. LNCaP cells were transfected with control or PHLDA3-targeting siRNAs and treated with adriamycin or 5-FU, which induces p53-dependent apoptosis (Figure S13). Upon treatment with the reagents, upregulation of p53 and p21 was observed (Figures 5C and 5D). PHLDA3 expression was effectively downregulated in cells transfected with siRNAs targeting PHLDA3 and, upon DNA damage, PARP cleavage and annexin V-positive/PI-negative cells were reduced, showing that PHLDA3 mediated DNA damage-induced apoptosis (Figures 5C–5E). Moreover, Akt activity was higher in cells with ablated PHLDA3 expression, indicating involvement of PHLDA3 in Akt repression upon DNA damage (Figures 5F and 5G). Taken together, these results demonstrate that PHLDA3 is required for p53-dependent apoptosis and Akt repression.

PHLDA3 Represses Akt under Basal Conditions

In addition to the effects of PHLDA3 knockdown upon p53 activation, we analyzed the effects under basal conditions. In PH3-sh cells infected with Ad-LacZ, elevated Akt phosphorylation was observed compared to ctrl-sh cells, showing that p53-independent basal PHLDA3 expression also inhibits Akt activation (Figure 5B, lane 1–3). Furthermore, as shown in Figure 5H, when control- and PH3-sh2 cells were transfected with GFP-PH-Akt, stronger localization of GFP-PH-Akt was observed in PH3-sh2 cells, further demonstrating the ability of PHLDA3 to inhibit Akt membrane translocation. In addition, we analyzed the effect of PHLDA3 knockdown under basal conditions in LNCaP cells (Figure 5I). It has been reported that Akt phosphorylates Mdm2 and increases Mdm2 activity to degrade p53 (Mayo and Donner, 2002). In PHLDA3 knocked-down cells, Akt and Mdm2 activities, elucidated by their phosphorylation, were increased (Figure 5I). Moreover, p53 levels were lower in these cells than control cells (Figure 5I and lanes 1–2 of Figures 5C and 5D); however, no such p53 decrease was observed when cells were treated with DNA-damaging agents, probably due to

(H) Ctrl-sh or PH3-sh2 cells were transfected with GFP-PH-Akt and treated with EGF for 5 min 24 hr post-transfection. Representative images of cells are shown in top panels. More than 150 cells were counted from three fields and classified into three groups: high, middle, or low GFP-PH-Akt at the plasma membrane. Percentage of cells with high GFP-PH-Akt localization at the membrane is shown in the bottom panel. The mean ± SD from three fields is shown.
(I) Control or PHLDA3-targeting siRNAs were introduced into LNCaP cells. Cells were harvested 72 hr post-transfection and analyzed by western blotting.

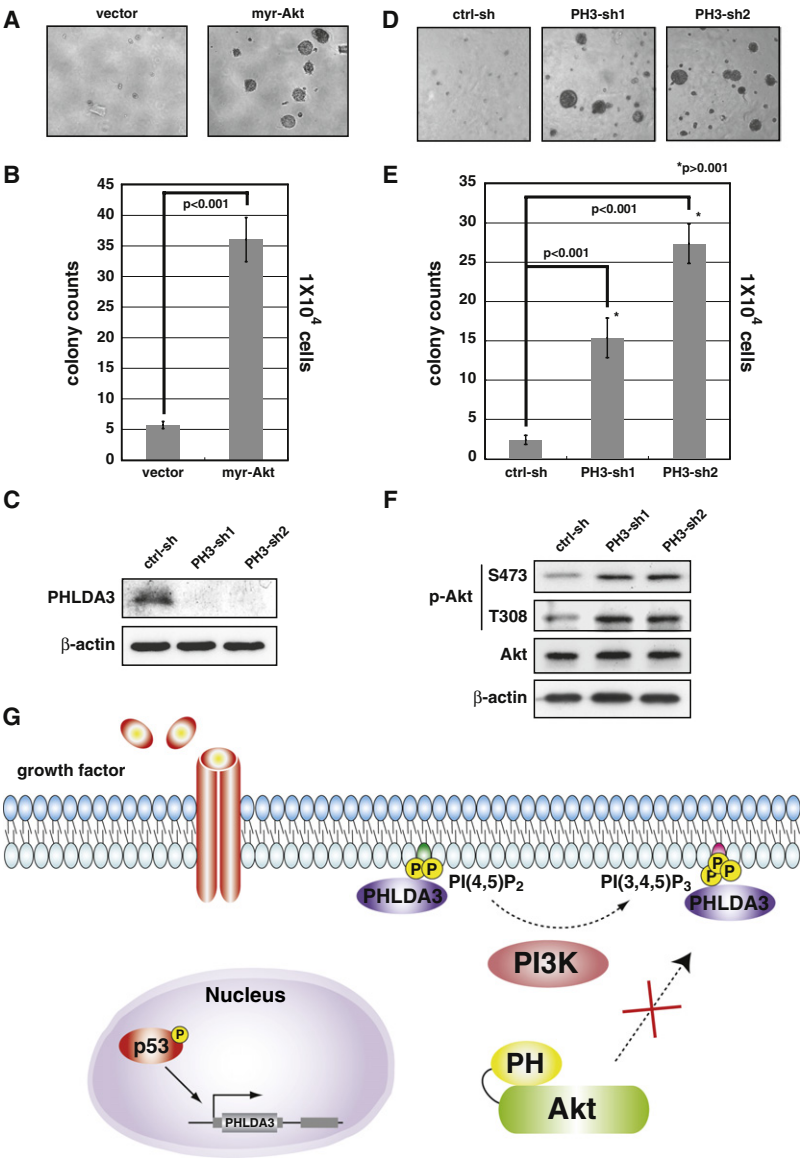

Figure 6. PHLDA3 Suppresses Anchorage-Independent Cell Growth

(A and B) Control and myr-Akt-expressing cells (1×10^4 cells) were plated in soft agar and cultured for 4 weeks. Colonies were analyzed by Image J software. Colonies were counted from three plates and the mean numbers of colonies ± SD are shown (B).

(C–F) Ctrl-sh, PH3-sh1, and PH3-sh2 cells were plated and analyzed as described above (D and E).

(C and F) PHLDA3 knock-down efficiency and Akt activity in colonies were analyzed. Whole-cell lysate (WCL) was prepared from colonies formed in soft agar from indicated cells and analyzed for PHLDA3 expression (C) and Akt activity (F) by western blotting.

(G) Novel Akt-inhibiting pathway downstream of p53 mediated by PHLDA3.

p53 phosphorylation protecting p53 against degradation by Mdm2 (lanes 3–6 of Figures 5C and 5D). These data demonstrate the complex mutual regulation of Akt and p53 and participation of PHLDA3 in the signaling cascade.

PHLDA3 Inhibits Anchorage-Independent Cell Growth

Since PHLDA3 mediated Akt inhibition without p53 activation, we further analyzed p53-independent function of PHLDA3. Akt is known to enhance anchorage-independent cell growth (Moore et al., 1998). We therefore analyzed whether PHLDA3 expression affects Akt-dependent colony formation in soft agar using MM468 cells without functional p53. In order to confirm Akt function in growth enhancement in soft agar, we first analyzed whether colony formation is enhanced in MM468 cells expressing myr-Akt. As shown in Figures 6A, 6B, and S14A, compared to control cells, cells expressing myr-Akt formed larger and more colonies in soft agar. We then analyzed the effect of PHLDA3 knockdown on colony formation efficiency. PHLDA3 expression under basal conditions or in cells forming colonies was analyzed and was almost undetectable in PH3-sh cells (Figures 6C and S14B). Similar to the results obtained with cells expressing myr-Akt, cells with ablated PHLDA3 expression formed larger and more colonies than ctrl-sh cells (Figures 6D, 6E, and S14C). When Akt phosphorylation levels of cells grown in soft agar were analyzed, those of PH3-sh cells were higher than those of control cells (Figure 6F). Taken together, PHLDA3 inhibited anchorage-independent cell growth and Akt activity independent of p53, suggesting a p53-independent role of PHLDA3 in tumor suppression.

The *PHLDA3* Gene Is Frequently Lost in Human Lung Endocrine Tumors

Inhibition of the Akt survival pathway is central to tumor suppression, and because PHLDA3 represses Akt in both p53-dependent and -independent manners, we considered that PHLDA3 might suppress human tumors. It has been reported that PI3K/Akt pathway activation is highly important for the oncogenicity of lung tumors (Engelman and Cantley, 2006). Accordingly, we performed comprehensive copy number analysis of primary human lung tumors (158 cases), 45 adenocarcinomas, 12 bronchioalveolar carcinomas, 52 squamous cell carcinomas, 8 small cell lung carcinomas, 29 LCNECs (large-cell neuroendocrine carcinoma), and 13 carcinoids, using a custom-made array spotted with 800 BAC clones (Peng et al., 2005; Shibata et al., 2005; and T.S., unpublished data). The *PHLDA3* gene is located in region 199.7 M chromosome 1, and because the most closely mapped BAC to *PHLDA3* in the array is that containing *PTPN7*, we judged chromosomal copy number changes of *PHLDA3* by copy number changes of BAC containing *PTPN7* (chromosomal locations of genes, Figure 7A). Interestingly, while no chromosomal alteration at the *PTPN7* locus was observed in adenocarcinoma, bronchioalveolar, squamous cell, and small-cell lung carcinoma, frequent chromosomal loss was

A

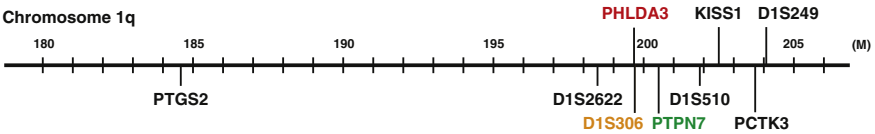

B

Locus x Sample	1T	2T	3T	4T	5T	6T	7T	8T	9T	10T	11T	12T
ABL2/1q24-1q25	0.86	0.88	1.00	1.24	1.26	0.94	0.97	1.19	0.78	1.16	0.87	1.33
LAMC2/1q25-1q31	0.98	1.02	1.13	1.36	1.49	1.09	1.09	1.54	0.85	1.25	0.92	1.64
TPR/1q25	1.25	1.46	1.57	1.77	2.06	1.53	1.56	2.17	1.10	1.80	1.25	1.87
PTGS2/1q25.2-1q25.3	1.15	1.41	1.40	1.50	2.12	1.33	1.48	1.64	0.96	1.36	1.15	1.68
PTPN7/1q32	0.69	0.61	0.77	0.96	1.05	0.75	0.92	0.93	0.78	0.84	0.79	1.15
PCTK3/1q31-1q32	0.70	0.63	0.79	1.03	0.98	0.79	0.77	1.21		0.99	0.74	1.06
KISS1/1q32	0.69	0.68	0.83	1.04	1.13	0.79	0.85	0.98		0.92	0.87	1.13
RBBP5/1q32	0.83	0.80	0.96	1.14	1.29	0.89	1.14	1.27	0.81	1.00	0.84	1.24
MDA7(IL24)/1q32	0.80	0.79	0.97	1.18	1.21	0.92	0.97	1.07	0.75	1.03	0.94	1.34
PPP2R5A/1q32	0.96	1.07	1.13	1.29	1.53	1.09	1.16	1.29	0.95	1.20	1.01	1.63
ATF3/1q32	0.80	0.79	0.92	1.19	1.13	0.91	0.92	1.17	0.73	0.95	0.86	1.25
PTPN14/1q32	0.93	1.09	0.82	1.30	1.51	1.08	1.39	1.25	0.87	1.19	0.94	1.45
CENPF/1q32	1.11	1.26	1.33	1.57	1.76	1.36	1.39	1.57	0.98	1.48	1.08	1.75
TGFB2/1q41	1.04	1.24	1.33	1.49	1.81	1.20	1.59	1.99	0.99	1.30	1.10	1.80

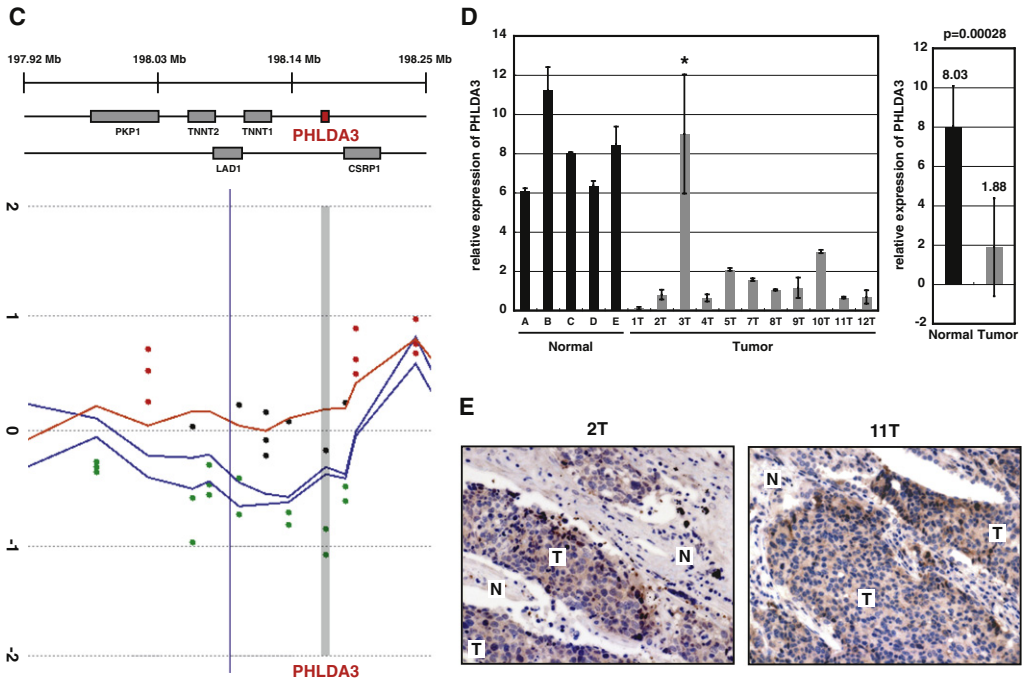

Figure 7. *PHLDA3* Locus Is Lost and PHLDA3 Expression Is Downregulated in LCNECs

(A) Chromosomal locations of *PHLDA3* gene, BACs used in CGH analysis, and microsatellite markers.

(B) Chromosome copy number alterations analyzed by MCG cancer array-800 CGH. When the signal ratio (test signal/reference signal) was less than 0.8, it was defined as chromosomal loss. Signal ratios less than 0.8 are in shaded boxes.

(C) Representative results of Agilent 44K CGH analysis on the *PHLDA3* gene locus in LCNEC samples. Chromosomal copy number ratio (tumor DNA/normal DNA) converted to log2 data at each oligonucleotide probe was plotted (green, red, and black spots indicate lost, amplified, and retained signals, respectively). The location of the *PHLDA3* gene locus is shown by a shaded column. Small chromosomal deletions, including *PHLDA3* locus, were detected in two LCNEC cases (blue lines, derived from patients L2 and L5, see Figure S15B), while no copy number loss was observed in the other case (red line, patient L17). Chromosome copy numbers shown by blue and red lines were calculated by applying a weighted moving-average window of 1 Mb.

(D) Expression of PHLDA3 was analyzed by quantitative RT-PCR. Total RNAs were prepared from normal lung tissues (derived from patients A–E) and LCNECs (derived from patients 1T–12T). PHLDA3 mRNA levels were analyzed as in Figure 1D. In the right column, the mean expression ± SD of PHLDA3 expression in normal lungs and tumor samples is shown.

(E) LCNEC tumor sections were subjected to immunohistochemistry to detect activated Akt. Stronger positive brown signals were detected in tumor regions (T) compared to normal tissue regions (N).

detected in LCNEC and carcinoid samples (11/29 LCNECs and 3/13 carcinoids showed chromosome loss at the PTPN7 locus, Figures 7B and S15A). In addition, we analyzed another cohort of 17 primary LCNECs with much higher resolution using the Agilent 44K oligonucleotide array, and 5 tumor samples showed deletion of the *PHLDA3* gene locus, further demonstrating the high frequency of chromosome loss at the *PHLDA3* locus in LCNECs (Figures 7C and S15B). To validate chromosome copy number alterations detected by comparative genomic hybridization (CGH), we next determined allelic loss in that region using microsatellite markers in 12 CGH-analyzed LCNEC samples. Five of six samples showing chromosomal loss by CGH analysis

concordantly revealed loss of heterozygosity (Figure S15C). Moreover, 3 of 6 samples showing no chromosomal loss by CGH analysis had allelic imbalance; therefore, collectively, 9 of 12 LCNECs had chromosomal abnormality at the *PHLDA3* locus.

We also analyzed p53 and PTEN status in 32 LCNEC samples (Figures S16A and S16B). The association between *PHLDA3* loss and WT genotype of PTEN was statistically insignificant ($p = 0.68$, by Fisher's exact test). PHLDA3 and PTEN inhibit the PI3K/Akt pathway by different mechanisms and, as shown for MM468 cells lacking PTEN, loss of PHLDA3 is additive to PTEN loss in Akt inhibition (Figures 4–6); therefore, it is reasonable that PTEN loss is not mutually exclusive to *PHLDA3* loss. On the other hand, while 63% (5/8) of tumors with WT p53 exhibited *PHLDA3* loss, only 13% (3/24) with nonfunctional p53 had *PHLDA3* loss; however, most likely due to the limited numbers of LCNEC samples, the association of *PHLDA3* loss and WT genotype of p53 was insignificant ($p = 0.088$).

Reduced PHLDA3 Expression and Elevated Akt Activation in LCNECs

We then analyzed whether such high frequency of chromosomal loss and aberration leads to abnormal PHLDA3 expression in tumors. As shown in Figure 7D, PHLDA3 expression was examined in 5 normal lung tissues and 11 CGH-analyzed LCNEC samples by quantitative RT-PCR. Except for one sample, obtained from a patient receiving chemotherapy prior to surgery (3T), all samples showed significant reduction of PHLDA3 expression. As we found no somatic mutation within the *PHLDA3* gene open reading frame in the 12 tumor samples described in Figures 7B and 7C (data not shown) and the highly reduced PHLDA3 expression in these tumors cannot be explained solely by hemizygous chromosome loss, *PHLDA3* locus in tumors might have undergone epigenetic changes, resulting in reduced PHLDA3 expression.

As a consequence of decreased PHLDA3 expression, we analyzed whether Akt activation occurs in these tumors. Immunohistochemistry of 32 LCNECs, including 10 tumors analyzed for PHLDA3 expression, revealed Akt activity levels in these tumors. Elevated phospho-Akt staining was detected in 27 tumor samples (including 9 analyzed for PHLDA3 expression), in which phospho-Akt staining was detected on the cellular membrane, cytoplasm, and nuclei (Figures 7E and S16). Taken together, these results indicate that PHLDA3 may exhibit a tumor-suppressing function in LCNECs through Akt inhibition.

DISCUSSION

PHLDA3 Is a PH Domain-Only Protein and an Akt Repressor

We have demonstrated that the *PHLDA3* gene is a direct target gene of p53. Although *PHLDA3* has been identified as a p53-inducible gene by several groups, this report is the first to identify *PHLDA3* as a direct target gene of p53 (Jen and Cheung, 2005; Kerley-Hamilton et al., 2005). Previously, the murine *PHLDA3* (also named *Tih1*) gene was cloned as the closest paralog of murine *Ipl*, also known as *PHLDA2* (Frank et al., 1999). The *Ipl* gene is expressed in the yolk sac, placenta, and fetal liver, while *PHLDA3* is expressed in multiple fetal and adult tissues, indicating that these two genes have nonoverlapping functions in development. In agreement, *Ipl* knockout mice showed placental overgrowth, confirming that at least one of *Ipl*'s biological functions is to regulate placental growth, while *PHLDA3* knockout mice did not show this phenotype (Frank et al., 2002). Both PHLDA3 and Ipl proteins are mostly composed of the PH domain. PIP binding analysis was performed using PH domains of PHLDA3 and Ipl proteins, and both bound to PIP with broad specificity for PIP (Figure 3C and Saxena et al., 2002); however, their physiological function remained unclear. Here, we showed that PHLDA3 functions as a PH domain-only protein and interferes with another PH domain-containing protein, Akt (Figure 6G).

It has been proposed that specific binding of PH domains to PIP is necessary but not sufficient to recruit the PH domain to the membrane, and alternative co-operative mechanisms are required (Lemmon and Ferguson, 2000; Maffucci and Falasca, 2001). It is also suggested that binding of PH domains to other membrane components, most probably proteins, is essential to enable specific participation in the regulation of specific signaling pathways (Varnai et al., 2005). In agreement, it has been reported that among PIP_3-binding PH domains, those of Btk, Akt, and Gab1 have Akt-inhibiting ability while those of Grp1 and ARNO do not (Ren and Wu, 2003; Varnai et al., 2005). Although it was shown that PIP_3 binding ability is required for Akt inhibition, not all PH domains that bind PIP_3 have Akt-inhibiting activity, indicating the importance of alternative co-operative mechanisms in selective functions of PH domains. PHLDA3 and the isolated PH domain of Akt similarly inhibited the Akt pathway but had almost no effect on the Grp1-regulated pathway, showing the selective function of PHLDA3 (Figure 3). Results by in vitro protein-lipid overlay assay demonstrated that PHLDA3 interferes with Akt binding to PIP directly (Figure 4F); however, alternative mechanisms may cause PHLDA3 to function specifically as a dominant-negative form of Akt, and it is an important future issue to determine whether such alternative mechanisms exist.

Functions of PHLDA3 in Lung Endocrine Tumors

By comprehensive analysis of human lung tumors using array-based CGH analysis, we found that the *PHLDA3* genomic locus is frequently lost in LCNECs and carcinoids, both of which are lung endocrine tumors. Lung endocrine tumors store and release small peptides and biogenic amines and are divided into four subtypes: (1) LCNEC, (2) carcinoid, (3) atypical carcinoid, and (4) small-cell lung cancer (Righi et al., 2007). Although lung endocrine tumors have certain uniform features on microscopy and immunohistochemical staining, they have a distinct incidence, epidemiology, and metastatic propensity and distinct clinical characteristics; therefore, defining their molecular and cellular characteristics is essential to improving diagnosis and therapy. The high incidence of loss of the *PHLDA3* genomic locus may account for a molecular characteristic of LCNECs and carcinoids. LCNEC has aggressive clinical behavior, showing poor prognosis and high affinity for distant metastasis (Righi et al., 2007). In addition, LCNEC was recognized rather recently, and therefore no efficient therapy has been established. It has been reported that nicotine and NKK (tobacco carcinogen) bind to nicotinic acetylcholine receptor and activate the Akt pathway

and contribute to tobacco-related carcinogenesis (West et al., 2003). Since LCNEC is directly related to smoking, our findings suggest that decreased expression of PHLDA3 may play an important role in the development and malignant progression of LCNEC. Accordingly, introducing efficient therapies for Akt repression may lead to a better prognosis for LCNEC patients.

In summary, we present a novel Akt-inhibiting pathway, in which Akt activity is inhibited by a PH domain-only protein, PHLDA3. Since PHLDA3 binds to various PIP, and there are numerous PH domain-containing proteins, further investigation will clarify whether PHLDA3 targets proteins other than Akt. Moreover, further detailed analysis of PHLDA3 abnormality in human cancers and tumor formation in *PHLDA3* knockout mice is necessary to assess the involvement of PHLDA3 in tumorigenesis.

EXPERIMENTAL PROCEDURES

For further detailed experimental procedures, please see the Supplemental Experimental Procedures.

ChIP-chip Assay and ChIP Sequence Analysis

For p53 induction, cells were treated with 5-FU (0.375 mM for 9 hr) and UV (10 J, harvested 9 hr post-irradiation). ChIP sequence analysis was performed on Illumina cluster station and 1G analyzer following the manufacturer's instructions.

p53 Pull-Down Assay by Biotinylated DNA Probe

Biotinylated probes were attached to streptavidin-magnetic beads and incubated with cell lysate prepared from p53-overexpressing H1299 cells.

Protein-Lipid Overlay Assay

Various phospholipids were spotted onto nitrocellulose membranes and incubated with purified proteins. Protein binding to the phospholipids was detected by enhanced chemiluminescence.

Cell Spreading and Cell Attachment Assay

Assay was performed as described (Varnai et al., 2005). COS7 cells were transfected with the indicated constructs for 24 hr. For the cell-spreading assay, cells were then plated on fibronection-coated chamber slides and harvested 20 min after plating. For the attachment assay, cells were divided into three aliquots, one of which was immediately harvested. The other two aliquots were plated and allowed to attach for 30 min. Attached cells were harvested and analyzed by western blotting.

Quantification of Cellular PI(3,4,5)P_3

PI(3,4,5)P_3 was quantified using a PIP_3 mass strip kit (Echelon Biosciences Inc., Salt Lake City, UT). Lipids were extracted from 3×10^6 MM468 cells infected with Ad-LacZ or Ad-PHLDA3, and cells were treated with LY294002 for 12 hr.

Array-Based Comparative Genomic Hybridization Analysis

BAC CGH array hybridization was carried out as described using MCG cancer array-800 (Peng et al., 2005). For higher-density oligonucleotide array CGH, we used Human Genomic CGH microarray 44B (Agilent Technologies, Palo Alto, CA).

SUPPLEMENTAL DATA

Supplemental Data include Supplemental Experimental Procedures, Supplemental References, and 16 figures and can be found with this article online at http://www.cell.com/supplemental/S0092-8674(08)01563-8.

ACKNOWLEDGMENTS

We are grateful to Atsushi Okabe for production of ChIP-chip and ChIP sequence data and Hiroko Meguro and Kaori Shiina for analysis of ChIP-chip and ChIP sequence samples. This study was supported by the program for the promotion of Fundamental Studies in Health Sciences of the Pharmaceuticals and Medical Devices Agency (to T.O. and H.I.), a Grant-in-Aid for Scientific Research and a grant of the Genome Network Project from the Ministry of Education, Culture, Sports, Science and Technology of Japan (to H.A.), a Grant-in-Aid for Scientific Research from the Ministry of Education, Culture, Sports, Science and Technology of Japan (to Y.T.), and a Grant-in-Aid for Third Term Comprehensive Control Research for Cancer from the Ministry of Health, Labor and Welfare, Japan (to T.S. and Y.T.). T.K. is a recipient of a research fellowship from the Japan Society for the Promotion of Science for Young Scientists.

Received: March 3, 2008
Revised: September 1, 2008
Accepted: December 3, 2008
Published: February 5, 2009

REFERENCES

Bode, A.M., and Dong, Z. (2004). Post-translational modification of p53 in tumorigenesis. Nat. Rev. Cancer *4*, 793–805.

Brooks, C.L., and Gu, W. (2006). p53 ubiquitination: Mdm2 and beyond. Mol. Cell *21*, 307–315.

Cully, M., You, H., Levine, A.J., and Mak, T.W. (2006). Beyond PTEN mutations: the PI3K pathway as an integrator of multiple inputs during tumorigenesis. Nat. Rev. Cancer *6*, 184–192.

Engelman, J.A., and Cantley, L.C. (2006). The role of the ErbB family members in non-small cell lung cancers sensitive to epidermal growth factor receptor kinase inhibitors. Clin. Cancer Res. *12*, 4372s–4376s.

Frank, D., Mendelsohn, C.L., Ciccone, E., Svensson, K., Ohlsson, R., and Tycko, B. (1999). A novel pleckstrin homology-related gene family defined by Ipl/Tssc3, TDAG51, and Tih1: tissue-specific expression, chromosomal location, and parental imprinting. Mamm. Genome *10*, 1150–1159.

Frank, D., Fortino, W., Clark, L., Musalo, R., Wang, W., Saxena, A., Li, C.M., Reik, W., Ludwig, T., and Tycko, B. (2002). Placental overgrowth in mice lacking the imprinted gene Ipl. Proc. Natl. Acad. Sci. USA *99*, 7490–7495.

Franke, T.F., Kaplan, D.R., Cantley, L.C., and Toker, A. (1997). Direct regulation of the Akt proto-oncogene product by phosphatidylinositol-3,4-bisphosphate. Science *275*, 665–668.

Harriague, J., and Bismuth, G. (2002). Imaging antigen-induced PI3K activation in T cells. Nat. Immunol. *3*, 1090–1096.

Harris, S.L., and Levine, A.J. (2005). The p53 pathway: positive and negative feedback loops. Oncogene *24*, 2899–2908.

Jen, K.Y., and Cheung, V.G. (2005). Identification of novel p53 target genes in ionizing radiation response. Cancer Res. *65*, 7666–7673.

Kawase, T., Ichikawa, H., Ohta, T., Nozaki, N., Tashiro, F., Ohki, R., and Taya, Y. (2008). p53 target gene AEN is an exonuclease required for p53-dependent apoptosis. Oncogene *27*, 3797–3810.

Kerley-Hamilton, J.S., Pike, A.M., Li, N., DiRenzo, J., and Spinella, M.J. (2005). A p53-dominant transcriptional response to cisplatin in testicular germ cell tumor-derived human embryonal carcinoma. Oncogene *24*, 6090–6100.

Lemmon, M.A., and Ferguson, K.M. (2000). Signal-dependent membrane targeting by pleckstrin homology (PH) domains. Biochem. J. *350*, 1–18.

Liu, G., and Chen, X. (2006). Regulation of the p53 transcriptional activity. J. Cell. Biochem. *97*, 448–458.

Luo, J., Manning, B.D., and Cantley, L.C. (2003). Targeting the PI3K-Akt pathway in human cancer: rationale and promise. Cancer Cell *4*, 257–262.

Maffucci, T., and Falasca, M. (2001). Specificity in pleckstrin homology (PH) domain membrane targeting: a role for a phosphoinositide-protein co-operative mechanism. FEBS Lett. *506*, 173–179.

Manning, B.D., and Cantley, L.C. (2007). AKT/PKB signaling: navigating downstream. Cell *129*, 1261–1274.

Mayo, L.D., and Donner, D.B. (2002). The PTEN, Mdm2, p53 tumor suppressor-oncoprotein network. Trends Biochem. Sci. *27*, 462–467.

Moore, S.M., Rintoul, R.C., Walker, T.R., Chilvers, E.R., Haslett, C., and Sethi, T. (1998). The presence of a constitutively active phosphoinositide 3-kinase in small cell lung cancer cells mediates anchorage-independent proliferation via a protein kinase B and p70s6k-dependent pathway. Cancer Res. *58*, 5239–5247.

Oda, E., Ohki, R., Murasawa, H., Nemoto, J., Shibue, T., Yamashita, T., Tokino, T., Taniguchi, T., and Tanaka, N. (2000). Noxa, a BH3-only member of the Bcl-2 family and candidate mediator of p53-induced apoptosis. Science *288*, 1053–1058.

Ohki, R., Nemoto, J., Murasawa, H., Oda, E., Inazawa, J., Tanaka, N., and Taniguchi, T. (2000). Reprimo, a new candidate mediator of the p53-mediated cell cycle arrest at the G2 phase. J. Biol. Chem. *275*, 22627–22630.

Ohki, R., Kawase, T., Ohta, T., Ichikawa, H., and Taya, Y. (2007). Dissecting functional roles of p53 N-terminal transactivation domains by microarray expression analysis. Cancer Sci. *98*, 189–200.

Oren, M. (2003). Decision making by p53: life, death and cancer. Cell Death Differ. *10*, 431–442.

Peng, W.X., Shibata, T., Katoh, H., Kokubu, A., Matsuno, Y., Asamura, H., Tsuchiya, R., Kanai, Y., Hosoda, F., Sakiyama, T., et al. (2005). Array-based comparative genomic hybridization analysis of high-grade neuroendocrine tumors of the lung. Cancer Sci. *96*, 661–667.

Ren, Y., and Wu, J. (2003). Simultaneous suppression of Erk and Akt/PKB activation by a Gab1 pleckstrin homology (PH) domain decoy. Anticancer Res. *23*, 3231–3236.

Righi, L., Volante, M., Rapa, I., Scagliotti, G.V., and Papotti, M. (2007). Neuroendocrine tumours of the lung. A review of relevant pathological and molecular data. Virchows Arch. *451*, 51–59.

Saxena, A., Morozov, P., Frank, D., Musalo, R., Lemmon, M.A., Skolnik, E.Y., and Tycko, B. (2002). Phosphoinositide binding by the pleckstrin homology domains of Ipl and Tih1. J. Biol. Chem. *277*, 49935–49944.

Scheid, M.P., and Woodgett, J.R. (2003). Unravelling the activation mechanisms of protein kinase B/Akt. FEBS Lett. *546*, 108–112.

Schneider, R., Bannister, A.J., Myers, F.A., Thorne, A.W., Crane-Robinson, C., and Kouzarides, T. (2004). Histone H3 lysine 4 methylation patterns in higher eukaryotic genes. Nat. Cell Biol. *6*, 73–77.

Shibata, T., Uryu, S., Kokubu, A., Hosoda, F., Ohki, M., Sakiyama, T., Matsuno, Y., Tsuchiya, R., Kanai, Y., Kondo, T., et al. (2005). Genetic classification of lung adenocarcinoma based on array-based comparative genomic hybridization analysis: its association with clinicopathologic features. Clin. Cancer Res. *11*, 6177–6185.

Songyang, Z., Baltimore, D., Cantley, L.C., Kaplan, D.R., and Franke, T.F. (1997). Interleukin 3-dependent survival by the Akt protein kinase. Proc. Natl. Acad. Sci. USA *94*, 11345–11350.

Stambolic, V., Mak, T.W., and Woodgett, J.R. (1999). Modulation of cellular apoptotic potential: contributions to oncogenesis. Oncogene *18*, 6094–6103.

Stokoe, D., Stephens, L.R., Copeland, T., Gaffney, P.R., Reese, C.B., Painter, G.F., Holmes, A.B., McCormick, F., and Hawkins, P.T. (1997). Dual role of phosphatidylinositol-3,4,5-trisphosphate in the activation of protein kinase B. Science *277*, 567–570.

Varnai, P., Bondeva, T., Tamas, P., Toth, B., Buday, L., Hunyady, L., and Balla, T. (2005). Selective cellular effects of overexpressed pleckstrin-homology domains that recognize PtdIns(3,4,5)P3 suggest their interaction with protein binding partners. J. Cell Sci. *118*, 4879–4888.

Vogelstein, B., Lane, D., and Levine, A.J. (2000). Surfing the p53 network. Nature *408*, 307–310.

Vousden, K.H., and Prives, C. (2005). p53 and prognosis: new insights and further complexity. Cell *120*, 7–10.

West, K.A., Brognard, J., Clark, A.S., Linnoila, I.R., Yang, X., Swain, S.M., Harris, C., Belinsky, S., and Dennis, P.A. (2003). Rapid Akt activation by nicotine and a tobacco carcinogen modulates the phenotype of normal human airway epithelial cells. J. Clin. Invest. *111*, 81–90.